（課程博士用）
(for Degree earned by Completing Doctoral Program)

千葉大学審査学位論文（要約）（Summary）

大学院融合科学研究科　情報科学専攻　知能情報コース
Graduate School　Division　Department

学生証番号　15YD1306
Student ID Number

氏　名 CAHYA EDI SANTOSA
Name

論文題名（外国語の場合は、その和訳を併記）
Thesis Title（foreign language title must be accompanied by Japanese translation）

航空機搭載Cバンド全偏波CP-SAR用広帯域円偏波マイクロストリップアレーアンテナの開発及び実装

Development and Implementation of The Broadband Circularly Polarized Microstrip Array Antenna for C-Band Full Polarimetric Airborne CP-SAR

Final Thesis Summary

Development and Implementation of The Broadband Circularly Polarized Microstrip Array Antenna for C-Band Full Polarimetric Airborne CP-SAR

Cahya Edi Santosa
15YD1306

Abstract—Currently, Chiba University is developing L, C, and X-band circularly polarized synthetic aperture radar (CP-SAR) system for global environmental and disaster monitoring. The CP-SAR system designed as the payload of the unmanned aerial vehicle (UAV), aircraft, and microsatellite. This thesis presents the development and implementation of the circularly polarized microstrip array antenna for C-band full polarimetric airborne CP-SAR. The objective of this research is to investigate the novel design of the broadband microstrip array antenna which has the optimum performance as the CN235MPA aircraft onboard CP-SAR sensor due to limitations of the available space and weight on the aircraft. The proposed microstrip antenna constructed of two stacked dielectric substrates with the proximity-stripline feeding network. A diagonally curve-truncation applied as a radiating patch element to generate the right-handed CP (RHCP) or left-handed CP (LHCP) radiation. The proposed antenna consists of 128 elements within the 8x16 array configuration. The dimension of the prototype antenna is 49.5 cm of length, 33.0 cm of width, 3.5 cm of thickness, and 2.3 kg of weight. The result of simulation using CST high-frequency EM simulator and measurement in the anechoic chamber shows a good agreement. The antenna had successfully implemented on CN235MPA aircraft in the Hinotori-C2 flight mission in Indonesia in March 2018 and succeed to produce a high-resolution full-polarimetric CP-SAR image with 400 MHz of bandwidth. The image becomes the first image of the full polarimetric CP-SAR in the World that could be used to derive axial ratio, ellipticity, tilt angle, and other information in the future.

1. INTRODUCTION

Recently, the Center for Environmental and Remote Sensing (CEReS), Chiba University, Japan, is developing L, C, X-band circularly polarized synthetic aperture radar (CP-SAR) system for environmental and disaster monitoring. The CP-SAR system designed as the payload of an unmanned aerial vehicle (UAV), airborne, and microsatellite [1–5]. As an onboard payload, the CP-SAR system has a strict requirement in capabilities and limitation of electronic and hardware design including the antenna module. Several challenges in onboard CP-SAR antenna development are a limitation in available space on the platform, weight, and power of radio frequency (RF). The CP-SAR antenna with excellent electrical performance and supported by physically superiority such as compact sizes, lightweight, low profile, low cost, and ease in fabrication have become highly desired attributes. The microstrip antenna is a potential candidate to realize the onboard CP-SAR antenna. Unfortunately, microstrip antennas have several limitations in electrical characteristics such as small gain, low efficiency, and limited bandwidth.

The objective of this work is to create a novel design of the microstrip array antenna which has the broad bandwidth, high gain, reasonable characteristics on radiation pattern, compact size, and lightweight, as the airborne CP-SAR antenna due to limitations of available space and weight on the

platform. The simple square patch with diagonally curve-truncation as radiating patch placed at the central part of the antenna to generates the circularly polarized radiation. The proximity-coupled microstrip-line technique applied as a feeding network. The broadening bandwidth of the antenna applies multi-resonant frequency, shifted feed line position, modified shape of the parasitic patch, and circle-slotted of the parasitic patch. The upper layer of the array antenna covered by the copper plate in order to reduce the undesired electromagnetic emission from the feeding network. The proposed antenna arranged of 128 elements in 8×16 array configuration with fully serial sequential rotation feeding network to increase the total gain and optimize the axial ratio bandwidth. The first element in the serial sequential rotation of each subarray arranged on their position to be central elements of the array pattern to concentrate the radiation power intensity at the center of the array. The proposed antenna designed has both RHCP and LHCP polarization to provide a full polarimetric of CP-SAR image.

2. RELATED WORK

As an active imaging radar, SAR transmits an electromagnetic wave and receives the scattering wave from an object on the beam footprint. The SAR system allows operated in all weather conditions such as cloudy, foggy, and day to night time [6]. Standard SAR systems apply linearly-polarized (LP) microwaves to perform LP-SAR image mode (VV, HH, VH, and HV) [7,8]. Unfortunately, LP-SAR pulse is sensitive to Faraday rotation when the microwave propagates through the ionosphere and consume high power corresponding with mismatched of polarization [9]. The orientation angle of the LP-SAR microwave changes and needs the effort to correct the error in image processing [10]. A CP microwave that generated and received by a CP antenna ignore the mismatched orientation of polarization so that effective to neglect the Faraday phenomena [2] [11].

2.1. Airborne SAR

Since the 1980s, the AIRSAR system (NASA) and the Canadian CV580 system (CSRS) has been starting in development of the airborne SAR system for a civilian application. The AIRSAR system uses a microstrip array antenna, and the CV580 system applies a horn antenna as the SAR sensor. After that, most SAR systems operated in a linear polarization and became fully polarimetric mode with multi-frequency configuration. Table 1 listed several airborne SAR system with the platform and main antenna parameters. Generally, the SAR antennas mount in the pods and installed under the fuselage or the wings of the platform. Hinotori C2 comes with the new concept in broad bandwidth in the circularly polarized mode with a fully polarimetric operation and in-house antenna development. The E/F-SAR system will be presented in more detail as a comparison for the Hinotori C2 system by considering the closeness in the similarity of the center frequency, antenna type, bandwidth, and platform type.

2.2. Circularly Polarized Microstrip Antenna

In Chiba University, several shapes of CP patch antennas ware proposed for CP-SAR application. Various design of single patch antennas to obtain the best performance of CP-SAR antennas depicted in Figure 1. All model of CP antennas including an elliptical, square patch with corner truncation, equilateral triangular, elliptical annular ring, elliptical annular ring with a sine wave periphery, and elliptical with triple fed are using proximity fed and designed for L-band CP-SAR application [12–16]. This technique aims to avoid the complexity of the feeding network in arraying design. Unfortunately, neither array design finished, or performances of all designed antennas do not fulfill the design requirement of the CP-SAR antenna. The main problem is the trade-off between antennas dimension with performances of antennas bandwidth, gain, and radiation pattern, are not meet the maximum setting. The comparison of measured performances of proposed antennas listed in Tabel 2.

Table 1. Overview of C-band Airborne SAR antenna.

MISSION NAME		AIRSAR	CV-580	EMISAR	E-SAR	F-SAR	RAMSES	HINOTORI C2
Agency		NASA	CCRS	DCRS	DLR		ONERA	Proposed
Country		USA	Canada	Danmark	Germany		France	Japan
Platform		DC-8	Convair 580	Gulfstream 3	Dornier 228		Transall C160	CN-235
Antenna		Microstrip	Horn	Microstrip	Microstrip		Microstrip	Microstrip
Frequency		C-band	C-band	C-band	C-band		C-band	C-band
Polarization		Linear	Linear	Linear	Linear	Linear	Linear	Circular
Polarimetric		Quad	Quad	Quad	Dual	Quad	Quad	Quad
Bandwidth (MHz)		40	34	100	100	384	300	400
Gain (dBi)		24	26	26	17	NA	NA	21.3
Beamwidth (Degree)	Az. (*H*-plane)	3.3	2.5	8	19	NA	2.4	6
	Rg. (*E*-plane)	25	50	33	33	NA	31	13

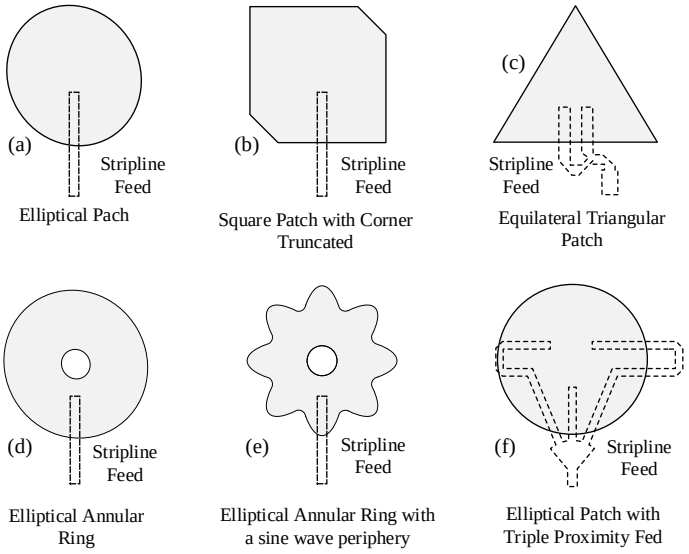

Figure 1. Proximity fed circularly polarized patch antenna [12–16].

Table 2. Various shape of patch antennas and their measured performance [12–16].

The Pacth Antenna Type	IBW (MHz)	ARBW (MHz)	Gain (dBic)
Elliptical	20	10.4	6.5
Square Patch with Corner Truncated (12 elements)	77	13.0	16.1
Equilateral Triangular	26	7.4	6.5
Elliptical Annular Ring	25	8.7	6.5
Elliptical Annular Ring with A Sine Wave Periphery	30	9.5	6.1
Elliptical Patch with Triple Proximity Fed (G)	34	8.7	7.2

3. METHODOLOGY

In this research, several activities such as designing, manufacturing, and measurement of microstrip array antenna does in the Center for Environmental and Remote Sensing (CEReS-Japan). The realized microstrip array antenna integrated with the CP-SAR system for ground-based test on the field and flight-test experiment using CN-235 aircraft in Jogjakarta and Makassar, Indonesia. Scanning mode of the CP-SAR system uses side looking mode with installing the antenna in full-polarimetric configuration (RR, LL, RL, and LR).

The conceptual design of impedance bandwidth (IBW) and axial ratio bandwidth (ARBW) of L-band CP-SAR antenna is 200 MHz for the airborne platform (JX-1 UAV) and 36 MHz for microsatellite platform (GAIA II satellite). For C-band and X-band airborne CP-SAR antenna, target specifications of IBW and ARBW are 400 MHz and 800 MHz, respectively [5]. The gain of antennas for airborne CP-SAR applications should be more significant than 20 dBic. For microsatellite CP-SAR applications, the gain of the antenna with parabolic reflector desired higher than 40 dBic.

4. THE ANTENNA DESIGN

The antenna of the airborne CP-SAR designed for RF transmitter (TX) and receiver (RX). The airborne CP-SAR system should have 4 unit array antennas to perform full polarimetric CP-SAR images (RR, RL, LR, and LL), that is 2 unit RHCP antennas and unit LHCP antennas. Figure 2(a) illustrates the layout of 4 unit CP-SAR array antennas that installed inside the nosecone of the CN-235 aircraft. The direction of the main beam of the antenna toward to nadir axis (N) is approximately 60°. Figure 2(b) shows the configuration of the full-polarimetric mode of the airborne CP-SAR sensor. Available space inside the nosecone of the aircraft is 100 cm of length in x-axis and 80 cm of width in y-axis. Limitation in space is a challenge for array antenna design to achieve the optimum performance of IBW, ARBW, and gain. The design requirement of the circularly polarized antenna in the conceptual design of the airborne CP-SAR system given in Table 3.

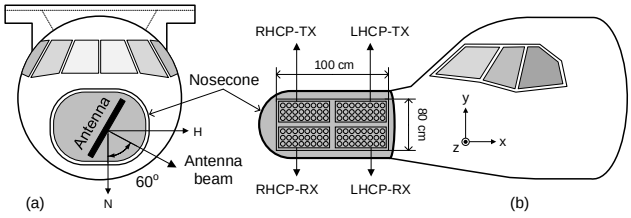

Figure 2. The layout of the airborne CP-SAR antenna that installed inside the nosecone of CN-235 aircraft. (a) The direction of the antenna (off-nadir-angle: 60°). (b) The configuration of the antenna for the full-polarimetric mode.

4.1. Single patch

The proposed antenna designed by a thick substrate with a low dielectric constant to broaden the IBW. To make thicker substrate, the proposed antenna constructed by stacking two layer NPC-H220A substrates with 1.6 mm thickness (h), 2.17 dielectric constant (ϵ_r), 0.035 mm copper-cladding thickness (t), and 0.0005 of dissipation factor (tan-δ). The designed structure of the single patch antenna shown in Figure 3(a) and 3(d) [17]. To simplify the design of the antenna, the shape of the radiating patch applies a square patch with diagonally curve corner-truncation and the feeding adopts a single-fed proximity-coupled strip line that placed between two substrates. On

Table 3. Design requirement of the C-band airborne CP-SAR antenna.

Parameters	Value	Unit	Parameters	Value	Unit
Center Frequency (f_c)	5.3	GHz	Cross Polarization	≤ -20	dB
-10dB Impedance Bandwidth (IBW)	400	MHz	Isolation	≤ -30	dB
3dB Axial Ratio Bandwidth (ARBW)	400	MHz	Tilt angle	25 – 60	Degree
Range Beam width (*E*-plane)	10	Degree	VSWR (1:2)	1 – 2	-
Azimuth Beam width (*H*-plane)	5	Degree	Input impedance (Z_{11})	50 + *j*0	Ohm
Total Gain (G)	≥ 20	dBic	Connector	N-type	-
Side-lobe-level (SLL)	≤ -20	dB	Antenna size ($x \times y \times z$)	500×300×10	mm

the upper layer of the top substrate, a parasitic patch with circle-slotted aligned with the center of the radiating patch. The parasitic patch with circle-slotted applies to improve the bandwidth and gain. To reduce an undesired electromagnetic field emitted by the feeding, most of the upper layer of the top substrate covered by copper. The bottom layer of the antenna structure is entirely a copper sheet that used as a ground plane.

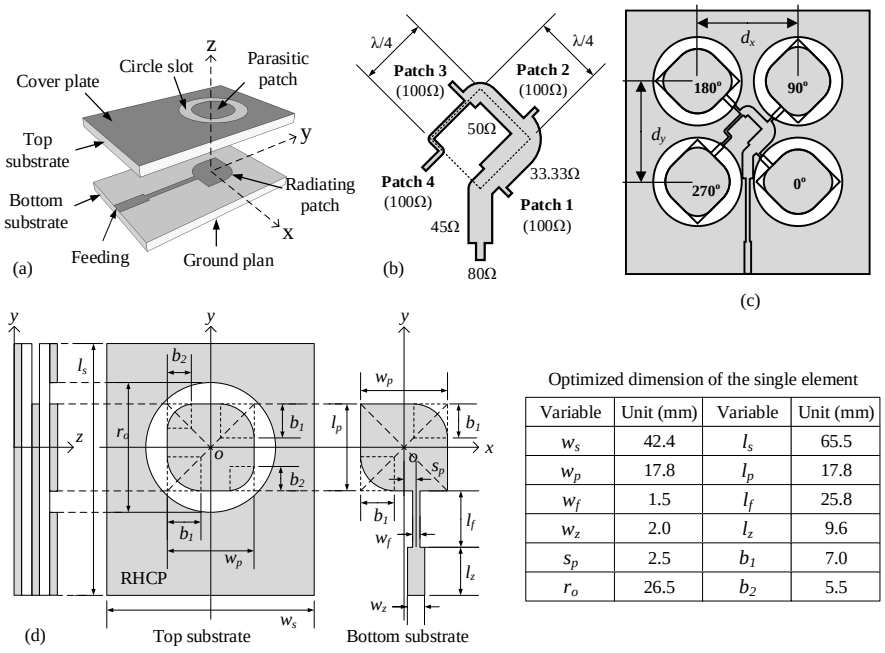

Optimized dimension of the single element

Variable	Unit (mm)	Variable	Unit (mm)
w_s	42.4	l_s	65.5
w_p	17.8	l_p	17.8
w_f	1.5	l_f	25.8
w_z	2.0	l_z	9.6
s_p	2.5	b_1	7.0
r_o	26.5	b_2	5.5

Figure 3. The structure of microstrip antenna. (a) Single patch construction. (b) Matching impedance for 2×2 configuration. (c) Geometry of 2×2 subarray configuration. (d) The detailed geometry of the optimized patch.

4.2. Sub-array Antenna

The subarray elements employ a 2×2 configuration that composed of four single patches with serial sequential rotation (SSR) technique as an effort to broaden the IBW and ARBW. The design of impedance matching for the 2×2 subarray feeding network with SSR configuration in the RHCP turn shown in Figure 3(b). Every subarray element (patch 1 until patch 4) fed by strip-line feeding

that matched to 100Ω. T-junction power divider applied to obtain a balanced power distribution toward each element of the subarray. The quarter lambda (λ/4) microstrip line used to shift the current phase between one patch to another patch become lagging 90° to each other to perform the SSR principles.

Figure 3(c) illustrates the configuration of 2×2 subarray for RHCP radiating patch antenna with patch separation d_x (in x-axis) and d_y (in y-axis).The patch separation among array elements is chosen between $0.5\lambda_o$ to $1.0\lambda_o$ to avoid unintended beam of the radiation pattern in the array antenna, where λ_o is a wavelength in free space [18]. For optimization study, several uniform patch separation (d_x=d_y) in $0.5\lambda_o$, $0.6\lambda_o$, $0.7\lambda_o$ are simulated and analyzed.

4.3. Full-array Antenna

The construction and dimension of 16×8 array antenna that employs the uniform patch separation with the SSR technique in RHCP mode shown in Fig.4. The bigger sub-array is 4×4 arranged by 4 sets of 2×2 sub-array configurations which each set of 2×2 sub-array applied the SSR principle in RHCP rotation. Every patch 1 (with phase 0°) of 2×2 sub-array placed as the center element of 4×4 sub-array configuration. Quarter-lambda phase shifter of 4×4 sub-array feeding network makes 90° phase differences between each patch in the center position (every patch 1 of 2×2 sub-array). This configuration performs a co-polarization rotation at the center element of 4×4 sub-array and cross-polarization between each set of 2×2 sub-array. Quarter-lambda phase shifter of 4×4 sub-array and 8×8 feeding network makes 90° phase differences between each set to perform the co-polarization rotation. The 16×8 array antenna is composed by dual 8×8 that combined by conventional corporate feeding network.

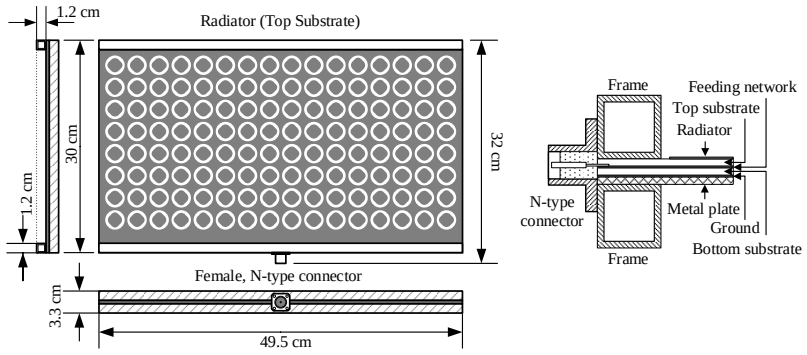

Figure 4. Structure of 16×8 microstrip array antenna.

4.4. Antenna Manufacturing and Measurement

Manufacturing and measurement activity is doing in the Center for Environmental and Remote Sensing (CEReS-Japan). The characteristics of the 16×8 array antenna had measured in the JMRSL anechoic chamber using E8364C PNA Microwave Network Analyzer as shown in Figure 5. The process of manufacturing and measurement use JMRSL laboratory tools and equipment. The method of etching process with the chemical process chosen in order to get a high accuracy of copper cladding removing. Two of microstrip array antennas of RHCP and two antennas of LHCP were independently manufactured and measured.

Table 4 summarize characteristics of the realized 16×8 antenna that both simulated and measured at the monitoring frequency of 5.3 GHz. Some measurement results were not following simulation results the simulations result due to specific errors in the fabrication and measurement process.

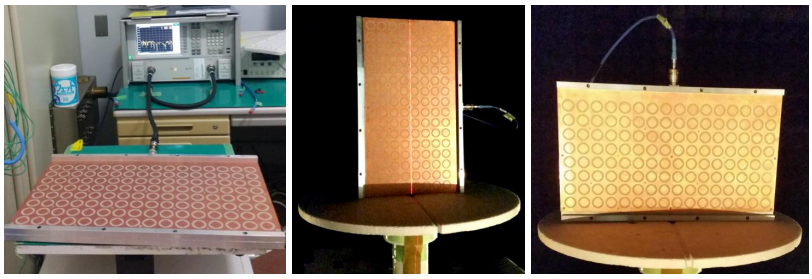

(a) (b) (c)

Figure 5. Characteristics measurement of the realized 16×8 antenna. (a) Return loss measurement. Radiation pattern and axial ratio measurements in (b) H-plane, and (c) E-plane.

Table 4. Characteristics of the 16×8 array antenna both simulated and measured at the frequency of 5.3 GHz with patch separation d_x=d_y=0.5λ_o.

Parameters		Value		Unit
		Simulation	Measurement	
Return-loss (S_{11})	f_L	4.54	4.94	GHz
	f_H	6.12	5.80	GHz
	IBW	1,580 (29.74)	860 (16.23)	MHz (%)
Axial-ratio (AR)	f_L	4.62	4.95	GHz
	f_H	6.64	6.27	GHz
	ARBW	2,020 (38.11)	1,330 (25.00)	MHz (%)
H-plane (ϕ=0°)	Direction	0.0	1.0	Degree
	BM	6.0	6.0	Degree
	SLL	-10.0	-8.57	dB
E-plane (ϕ=90°)	Direction	0.0	-1.0	Degree
	BM	13	13	Degree
	SLL	-15.8	-13.5	dB
Gain		23.7	21.3	dBic
VSWR (1:2)		1.39	1.22	None
Input Impedacne (Z_{11})		51.20+*j*1.72	55.16–*j*6.76	Ohm
Dimension ($x \times y$)		495×300×33	495×300×35	mm

5. INTEGRATION AND IMPLEMENTATION OF THE CP-SAR ANTENNA

5.1. Ground-based test

The geometrical layout for the ground base test illustrated in Figure 6. The CP-SAR system placed on the moving robot that has the path (r_y) along 50 m as an azimuth range. The 16×8 antenna placed 2.25 m hight on the ground and separated 1.5 m length between the transmitter (TX) and the receiver antenna (RX). As a point target, two trihedral corner reflectors with 0.75 m diameter placed 1.25 m hight on the ground at 95 m of range distance (r_x) from the antenna position. The range distance between first corner reflector and second corner reflector is 5 m (d_x), and the azimuth distance of them is 1 m (d_y). The moving robot controlled by the controller to move every 10 cm for transmitting pulse to the target and receive the scattering signal from the target.

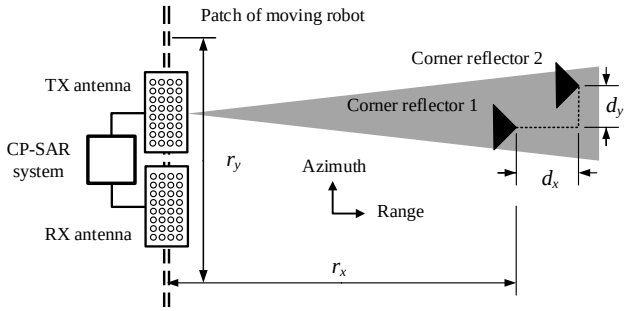

Figure 6. The layout of CP-SAR ground base experiment.

5.2. Flight-base test: Hinotori-C2 mission

The realized installation of the CP-SAR electronic hardware and the antenna shown in Figure 7. The electronic hardware of the CP-SAR system stacked up and placed on the back side of the pilot inside the CN-235 MPA cabin. The UPS and workstation battery placed on the bottom of the stacked up CP-SAR system. The timing and control unit (TCU) placed between the RF transmitter module and RF receiver module at the stacked up construction to minimize the effect of RF interference between TX and RX if any leakage. The IMU module placed on the top of the stacked up CP-SAR system and the GPS receiver mounted at the windows of the aircraft. The total weight of the electronic hardware of the CP-SAR system is about 80 kg.

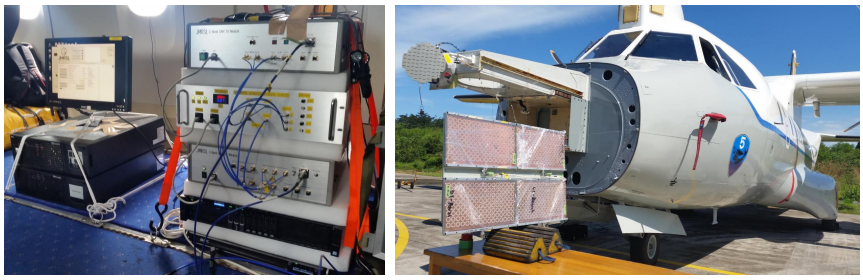

(a) (b)

Figure 7. (a) The electronic hardware of the CP-SAR installed inside the CN-235 MPA. (b) The position of the CP-SAR antenna during the point target test with the platform.

5.3. The result of the CP-SAR image

Figure 8 illustrated the scanning image of the CP-SAR system on flight path B2. This image generated by the CP-SAR system with an LR combination using four units of 16×8 array antenna and apply 400 MB chirp bandwidth. The image that marked with number 01 and 02 is the zoom in of the image that indicated by squared area number 01 and 02, respectively. The image shows the contrast between the backscattering signal from vegetation, land surface, and human-made building. The complete contrast forms the object inside the squared area 02 is possible to interpret and recognize the object. The proposed airborne CP-SAR antenna has proven to obtain the high-resolution image of CP-SAR with 37.5 cm resolution [19].

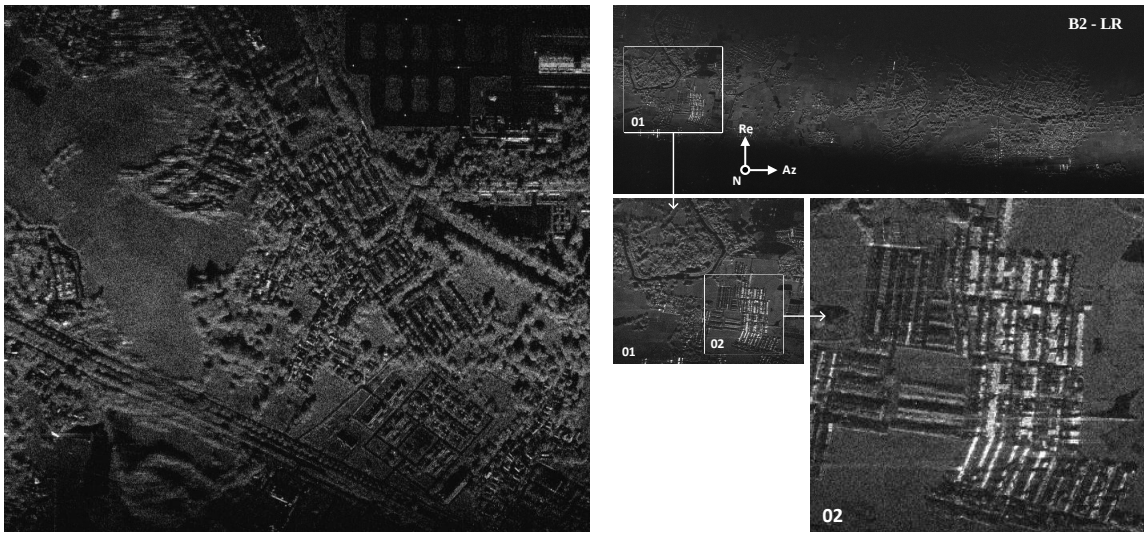

(a) (b)

Figure 8. High resolution of CP-SAR image that produced by (a) 200 MHz and (b) 400 MHz bandwidth of CP-SAR system and using the 16×8 antenna.

6. CONCLUSION

All of the proposed antennas have designed, simulated, manufactured, and measured at Chiba University. The measured peak gain of four prototype antenna obtained over than 20 dBic at the operational frequency of 5.1 GHz to 5.5 GHz. The prototype antenna has dimension 49.5 cm of length, 33.0 cm of width, and 3.5 cm of thickness, which has 2.3 kg of weight each antenna. The total weight of four unit antennas and their mounting installation is less than 20 kg and fit installed inside the nosecone of CN-235 MPA. The prototype antenna had successfully implemented on CN235 MPA in Hinotori-C2 flight mission in Makasar (Indonesia) in March 2018. The flight test mission succeeds to produce a high-resolution full-polarimetric CP-SAR image with 200 MHz and 400 MHz of bandwidth. The image becomes the first of full polarimetric CP-SAR image in the World. In the future, information about the axial ratio, ellipticity, tilt angle, and others can be derived from the CP-SAR data.

Four prototype antennas have successfully implemented on CN235 aircraft to perform the full polarimetric mode of CP-SAR in Hinotori-C2 flight mission in Makasar (Indonesia) in March 2018. The flight test mission succeeds to produce a high-resolution full-polarimetric CP-SAR image with 400MHz of bandwidth. The image becomes the first of full polarimetric CP-SAR image in the World and could be used to derive axial ratio, ellipticity, and tilt angle in the future.

REFERENCES

1. J.T. Sri Sumantyo, "Development of Circularly Polarized Synthetic Aperture Radar Onboard Microsatellite for Earth Diagnosis," in *IEEE International Geoscience and Remote Sensing Symposium (IGARSS)*, pp. 929-932,2011
2. J.T. Sri Sumantyo, "Development of Circular Polarized Synthetic Aperture Radar Onboard Unmanned Aerial Vehicle (CP-SAR UAV)," in *IEEE International Geoscience and Remote Sensing Symposium (IGARSS)*, pp. 4762-4765, 2012.
3. J.T. Sri Sumantyo, K. V. Chet, "Development of Circular Polarized Synthetic Aperture Radar

Onboard UAV for Earth Diagnosis," in *9th European Conference on Synthetic Aperture Radar(EUSAR)*, pp. 136-138, 2012.

4. J.T. Sri Sumantyo., V.C. Koo, T.S. Lim, T. Kawai, T.Ebinuma, Y.Izumi, M.Z. Baharuddin, S.Gao, and K.Ito, "Development of Circular Polarized Synthetic Aperture Radar Onboard UAV JX-1," in *International Journal of Remote Sensing*, Vol. 38, pp. 2745-2756, 2017.
5. J.T. Sri Sumantyo and N. Imura, "Development of Circular Polarized Synthetic Aperture Radar For Aircraft and Microsatellite," in *IEEE International Geoscience and Remote Sensing Symposium (IGARSS)*, pp. 5654-5657, Beijing, China, 2016.
6. Curlander, J.C.,and R.N. McDonough. *Synthetic Aperture Radar System and Signal Processing*, in A John Willey and Sons. Inc, Canada, 1991
7. Ouchi, K., "Recent Trend and Advance of Synthetic Aperture Radar with Selected Topics," in *Remote Sensing*, pp. 716-807, 2013.
8. Catalog of satellite instruments, *CEOS EO Handbook*, [Online] http://www.eohandbook.org, October 2018.
9. Gail, W. B., "Effect of Faraday Rotation on Polarimetric SAR," *IEEE Int. Transaction on Aerospace and Electronic System*, Vol.34, pp. 301-307, 1998.
10. H. Yang, J. H. An, H. W. Jung, and J. H. Kim, "Circular Polarization Implementation on Synthetic Aperture Radar," *2014 International Conference on Information and Communication Technology Convergence (ICTC)*, Busan, South Korea, 22-24 Oct 2014. pp. 991-994.
11. Gao, S., Q. Luo, F. Zhu, *Circularly Polarized Antenna*, John Willey Sons, 2014.
12. M. Baharuddin, V. Wissan, J.T. Sri Sumantyo, and H. Kuze, "Equilateral Triangular Microstrip Antenna for Circularly Polarized Synthetic Aperture Radar," *Progress in Electromagnetics Research C*, Vol.8, pp. 107-120, 2009.
13. M. Baharuddin, V. Wissan, J.T. Sri Sumantyo, and H. Kuze, "Development of An Elliptical Annular Ring Microstrip Antenna with Sine Wave Periphery," *Progress in Electromagnetics Research C*, Vol.12, pp. 27-36, 2010.
14. M. Baharuddin, V. Wissan, J.T. Sri Sumantyo, and H. Kuze,"Elliptical microstrip antenna for circularly polarized synthetic aperture radar," *International Journal of Electronics and Communications*, Vol.65, pp. 62-67, 2011.
15. Yohandri, V. Wissan, I. Firmansyah, P. Rizki Akbar, J.T. Sri Sumantyo, and H. Kuze, "Development of Circularly Polarized Array Antenna for Synthetic Aperture Radar Sensor Installed on UAV," *Progress in Electromagnetics Research C*, Vol.19, pp. 119-133, 2011.
16. Yohandri, J.T. Sri Sumantyo, and H. Kuze,"SA new triple proximity-fed circularly polarized microstrip antenna," *International Journal of Electronics and Communications*, Vol.66, pp. 395-400, 2012.
17. Santosa, C.E., J.T.S. Sumantyo, "Development of A Low Profile Wide-Bandwidth Circularly Polarized Microstrip Antenna for C-Band Airborne CP-SAR Sensor," in *Progress In Electromagnetics Research C*, Vol. 81, pp. 77-88, 2018.
18. Hansen, R.C.,*Phased Array Antennas*, John Willey and Sons, 1998.
19. J.T.Sri Sumantyo, M. Y. Chua, C. E. Santosa, G. F. Panggabean, T. Watanabe, B. Setiadi, F. D. Sri Sumantyo, K. Tsushima, K. Sasmita, A. Mardiyanto, E. Supartono, E. T. Rahardjo, G. Wibisono, R. H. Jatmiko, Sudaryatno, T. H. Purwanto, B. S. Widartono, M. Kamal, D. Perissin, S. Gao, and K. Ito, "Hinotori-C2 Mission: Airborne Circularly Polarized Synthetic Aperture Radar (CP-SAR)," *IEEE Transaction on Geoscience and Remote Sensing*, Submitted 15 September 2018.